Hindawi Publishing Corporation
Mathematical Problems in Engineering
Volume 2014, Article ID 608208, 12 pages
http://dx.doi.org/10.1155/2014/608208

Research Article

Experimental Evaluation of Novel Master-Slave Configurations for Position Control under Random Network Delay and Variable Load for Teleoperation

Ahmet Kuzu,[1,2] Seta Bogosyan,[1,3] Metin Gokasan,[1] and Asif Sabanovic[4]

[1]*Control Engineering Department, Faculty of Electrical and Electronics Engineering, Istanbul Technical University, 34469 Istanbul, Turkey*
[2]*Tubitak Bilgem BTE, 41470 Kocaeli, Turkey*
[3]*Electrical and Computer Engineering, University of Alaska Fairbanks, Fairbanks, AK 99775, USA*
[4]*Faculty of Engineering and Natural Sciences, Sabancı University, Orhanlı, Tuzla, 34956 Istanbul, Turkey*

Correspondence should be addressed to Ahmet Kuzu; kuzuah@itu.edu.tr

Received 13 June 2014; Revised 12 November 2014; Accepted 14 November 2014; Published 24 December 2014

Academic Editor: Hector Puebla

This paper proposes two novel master-slave configurations that provide improvements in both control and communication aspects of teleoperation systems to achieve an overall improved performance in position control. The proposed novel master-slave configurations integrate modular control and communication approaches, consisting of a delay regulator to address problems related to variable network delay common to such systems, and a model tracking control that runs on the slave side for the compensation of uncertainties and model mismatch on the slave side. One of the configurations uses a sliding mode observer and the other one uses a modified Smith predictor scheme on the master side to ensure position transparency between the master and slave, while reference tracking of the slave is ensured by a proportional-differentiator type controller in both configurations. Experiments conducted for the networked position control of a single-link arm under system uncertainties and randomly varying network delays demonstrate significant performance improvements with both configurations over the past literature.

1. Introduction

Teleoperation and bilateral control systems have been attracting significant interest due to their potential to contribute to human life, that is, teleoperated robots that contribute to safety and security in hazardous environments or exploration in remote areas or medical robots that can perform telesurgery [1]. Irrespective of the application, bilateral control is faced, to some extent, with problems resulting from uncertainties on the slave side and unpredictable network delays, which becomes significant when the Internet is used as the communication media.

Numerous studies have been performed for time delay compensation in bilateral control systems. The scattering variables approach [2] is a passivity based approach, using transmission line theories. In this approach, the data transfer between systems is designed in a way to avoid losses, hence ensuring passivity. The method has been initially designed for constant delay and further extended to variable delay. However, although stability is guaranteed according to the passivity theory, no transparency analysis is provided with the scattering variables method. The wave variables method in [3] is also derived from the scattering variables theory, based on the addition of a damping term to ensure stability in terms of passivity. However, in this method, transparency and stability are conflicting performance parameters. This issue is often addressed by the adaptive tuning of damping.

Optimal control methods have also been implemented to bilateral control with an aim to compensate for time delay while seeking an optimal solution for the stability and performance requirements of the system [4, 5]. Among other studies in the area, one can mention [6] with 2

types of PD controllers, [5] using L2 stability, [7] using multirate sampling, [8] on transparency and contact stability for single-master, multiple-slave telemanipulation, and [9] for the master- slave control of a multifingered humanoid by feeling the finger-tip force. There are also neural network based teleoperation studies as in [10, 11].

There are also sliding-mode control (SMC) approaches as in [12, 13]. The SMC based studies often consider the delay effects as a disturbance, hence seeking ways to make the system robust to such disturbances via control. In the field of medicine, for example, there is active research on time-delay compensation using SMC framework [14]. Other examples are [15], which uses SMC as a base for developing an efficient and robust adaptive fuzzy controller; in [16], equivalent control based SMC is used mainly for control delay compensation; in [17] the master control is performed via an impedance controller and the slave control via SMC controller. A recent study has proposed an SMC framework to simplify the interpretation of tasks in a multibody mechanical system, applicable to bilateral and multilateral control [18]. Sliding-mode control (SMC) based approaches in bilateral control often consider the delay effects as a disturbance, hence seeking ways to make the system robust to such disturbances via control. The well-known chattering problem associated with SMC systems can only be reduced with very high switching frequencies, which naturally conflicts with the conditions of time delay systems. To address this issue, chattering-free SMCs are proposed, but the high gain requirement of such systems is a major cause for instability under time delay conditions, yielding an acceptable performance mostly under short time delay (shorter than the sampling interval).

Smith predictor (SP) based applications mentioned above perform time delay compensation by using the system model and time delay model. The standard Smith predictor [19] will provide a good performance under known model and delay conditions, but will perform very poorly under random network delay, model, and load uncertainties, inherent to bilateral control systems. Astrom's Smith predictor [20] is proposed to improve SP's performance to some extent in the face of uncertainties; however, for an acceptable performance in bilateral control applications like the one under consideration, additional measures should be taken for delay regulation and disturbance rejection.

A more recent approach in bilateral control is the consideration of the communication delay effect as a disturbance, which is further addressed by the design of an observer, namely, a communication delay observer (CDOB). The method is shown to be more effective than the Smith predictor approach due to its independence of modeling errors and capability to handle variable delays as normally expected with the Internet. Moreover this method is as applicable to a SISO system as it is to MIMO systems [21, 22]. The CDOB approach lumps the delays in the control and measurement loop and proposes a 1st-order observer derived under the assumption of a linear system. The approach is based on the empirical determination of the cutoff, g, and, more recently, of the time constant, T. Although performing well under constant delay, the authors mention ongoing problems in practical applications under variable time delay and slave uncertainties.

This paper builds on the disturbance observer approach [12, 13] taken for the solution of network delays in bilateral control and aims to address specifically the variable delay, variable load, and model mismatch problems of [12, 13].

The main contribution of this study is developing and practically implementing two novel master-slave system configurations that yield a significantly improved performance in position control. Each configuration consists of a delay regulator integrated with disturbance rejection schemes on both master and slave sides. More specifically, the following two configurations are developed and tested under variable network delay and the model mismatch problems of bilateral control systems: (1) sliding mode observer (SMO) to compensate for measurement delay on the master side and a model tracking controller (MTC) on the slave side to reduce the effects of load uncertainties and model mismatch between master and slave; (2) Astrom's Smith predictor (ASP) to compensate for the effects of network delay on the master side and MTC against slave side uncertainties. Both configurations use the same delay regulator approach [23], which contributes significantly to the disturbance rejection performances of the SMO and ASP, as will be demonstrated with experimental results.

The proposed observer-regulator-controller configurations are tested for step type and bidirectional type load and reference trajectories under random network delays. Throughout the experiments, the emulated random delay is varied between 100 and 400 milliseconds, based on the network delay measured in [24], for a networking implementation between country-region France and place country-region USA using UDP/IP Internet protocol.

The organization of the paper is as follows. Section 2 presents the problem focused on. Sections 3, 4, and 5 discuss the functional blocks used in proposed topologies, delay regulator, estimation schemes, and model tracking control consequently. Section 6 shows their experimental results, with conclusions and future directions in Section 7.

2. System Configuration

The general configuration of the master-slave system considered in this study is given in Figure 1.

In this master-slave configuration, the human operator forces the master manipulator, which is in compliance mode, and generates a reference trajectory on the master side. This reference trajectory, together with the trajectory data coming from the slave side through the Internet, is considered by the master controller in the generation of the control signal that is generated to be sent to the slave side. On the slave side, the control signal coming from the master side through the Internet and the actual slave trajectory data is processed by the slave controller and actual control signal is generated. The information sent from the master side to the slave side is a message package containing the tapped control input signal (the reference current value) and a sequence ID. On slave side, more specifically, on the received side of the slave regulator, this information is processed to get the actual current input

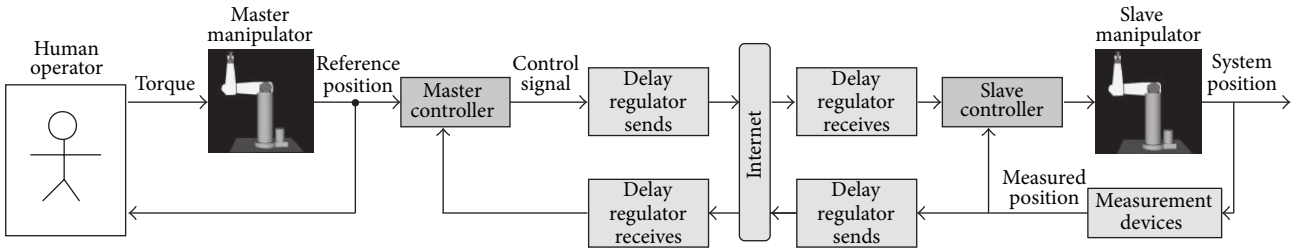

Figure 1: Configuration of the bilateral control system with communication delays both in control and feedback paths.

signal to be applied as reference to the slave side. As a result of this process, the input current signal is now compensated for data losses and the delay is regulated to a constant value.

The equation of motion for a direct-drive single link arm with load can be given as follows:

$$\dot{\theta}(t) = \omega(t), \tag{1}$$

$$\dot{\omega}(t) = \frac{K_t}{J}u(t) - \frac{B}{J}\omega(t) - \frac{T_L}{J}, \tag{2}$$

where K_t is torque constant (N-m/A), J is system inertia (kg-m^2), B is viscous friction (N-ms/rad), $u = i_q$ is control current (A), and T_L is the gravitational load.

3. Design of Delay Regulator

For bilateral control systems using the Internet as the communication medium, it is necessary to consider the delay characteristics of different Internet protocols. Currently, the more commonly used IPs (Internet protocols) are the transport control protocol (TCP/IP) and the user datagram protocol (UDP). TCP provides a point-to-point channel for applications that require reliable communication. It is a higher-level protocol that manages to robustly string together data packets, sorting them and retransmitting them as necessary to reliably retransmit data. Further, TCP/IP is confirmation based; that is, it transmits data and waits for confirmation from the other side. If not fulfilled, it retransmits the data. With TCP/IP, there is no data loss.

The UDP protocol does not guarantee communication between two applications on the network. While TCP/IP is connection based, UDP is just a simple serial communication channel. Much like sending a letter through mail, and unlike TCP/IP, UDP does not confirm arrival, hence eliminating data retransmission. On the other hand, while its faster transmission rate may make UDP more preferable for most real-time control applications, some delay regulation measure is also necessary to minimize the data loss.

The delay regulator works are based on the following principle: each transmitted UDP packet consists of the current plus 31 previous data samples, in addition to a sequence ID. Once transmitted to the slave side, this packet is stored into a memory cell identified by the packet's sequence ID. The number of stored packets on the receiving end is limited with the buffer size, N. During the very first send-receive process, stored packets are not fed to the related control process (to master for feedback or to slave for control) until a selected $L < N$ threshold is reached. This L/T value determines the selected regulation period, which when exceeded, the first data, $x(k)$, is fed to related control process, and this memory cell is labelled as null($\varnothing$). In the next sample time x_{k+1} will be fed to the control process until we face a data loss, in which case x_{k+2} will be null. In this case the algorithm checks the next memory cell and then the next one until a noncorrupted x_{k+2} value is founded in the memory cells below [23, 25]. The figure of a sample signal flow is seen in Figure 2.

4. Design of Control and Estimation Schemes for the Master-Slave System

Two control approaches are developed for the master side: one based on Smith predictor principles and one using sliding mode concepts. A discussion of both will be provided in this section.

4.1. Astrom's Smith Predictor on Master Side. The Smith predictor (SP) concept [19] is based on the design of a controller that can predict how the effects of system changes will affect the controlled variable (system output) in the future. The standard SP configuration, which requires the time delay to be constant (or known), has the shortcoming of poor disturbance rejection. Watanabe' Smith predictor (WSP) [26] and Astrom's Smith predictor (ASP) [20], given in Figure 3, have been proposed to overcome this problem. While both ASP and WSP are two degree of freedom modified Smith predictors, here we prefer Astrom's Smith predictor because, contrary to Watanabe's Smith predictor, effect of auxiliary controller does not degrade main controller performance [20].

Astrom's Smith predictor (ASP) decouples the disturbance response from the reference response, allowing the two to be independently optimized. Furthermore, its structure provides the designer with more freedom to choose the transfer function, $M_{\text{asp}}(s)$. Considering the developed delay regulator and the slave-side disturbance rejection scheme (to be discussed in the next section), an ASP based master control appears to be well suited for the targeted performance standards in this study. Within this configuration, the human operator generates the master trajectory, which then leads to the generation of the control input current to be transmitted to the slave side as explained in Section 2. At the slave side, the delayed control signal coming from the master side

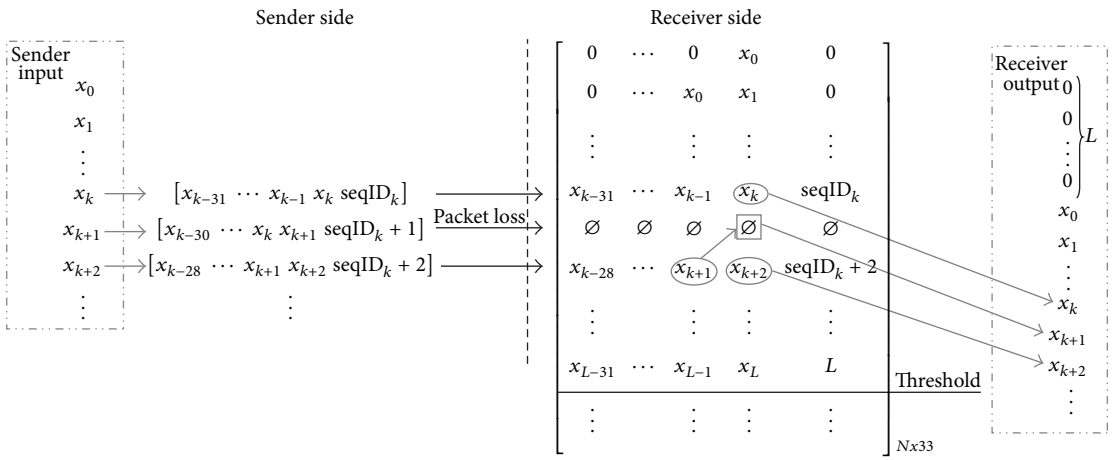

Figure 2: Delay regulator sample signal flow diagram.

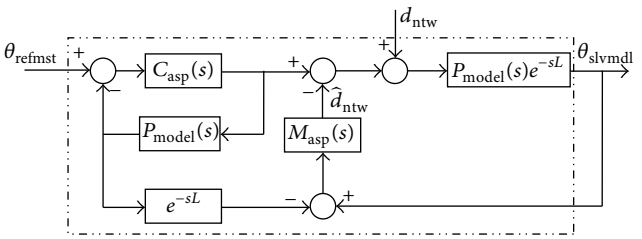

Figure 3: Astrom's Smith predictor.

(through the Internet) and the actual slave feedback data are processed by the slave controller and the actual control signal is generated and applied to the slave. The ASP is expected to compensate for disturbances caused by communication discrepancies between master and slave, when the buffer side is exceeded. Figure 3 presents the designed ASP within the proposed master-slave.

For the determination of the transfer function, $M_{asp}(s)$ of the ASP, the reference-to-output and disturbance-to-output transfer functions should first be taken into consideration for the system. With the given structure and with the assumption that the delay is constant, L, the reference-to-output transfer function will be independent of $M_{asp}(s)$ [27, 28]:

$$\frac{\theta_{slvmdl}(s)}{\theta_{refmst}(s)} = \frac{C_{asp}(s)\,P_{model}(s)\,e^{-sL}}{1 + C_{asp}(s)\,P_{model}(s)} \times \frac{1 + M_{asp}(s)\,P_{model}(s)\,e^{-sL}}{1 + M_{asp}(s)\,P_{model}(s)\,e^{-sL}}, \quad (3)$$

$$\frac{\theta_{slvmdl}(s)}{\theta_{refmst}(s)} = \frac{C_{asp}(s)\,P_{model}(s)\,e^{-sL}}{1 + C_{asp}(s)\,P_{model}(s)}.$$

Here C_{asp} is the main controller whose parameters are designed by ignoring network delay. In this work we choose C_{asp} as a PID controller whose parameters are k_{PCasp}, k_{ICasp}, and k_{DCasp}.

On the other hand, the disturbance response is as follows:

$$\frac{\theta_{slvmdl}(s)}{d_{ntw}(s)} = \frac{P_{model}(s)\,e^{-sL}}{1 + M_{asp}(s)\,P_{model}(s)\,e^{-sL}}, \quad (4)$$

where

$$P_{model}(s) = \frac{K_{tn}}{s\left(J_n s + B_n\right)}. \quad (5)$$

Also K_{tn}, J_n, and B_n are the rated parameter values of K_t, J, and B, respectively.

To suppress the disturbance $\widehat{d}_{ntw}$ should track d_{ntw} in Figure 3. The transfer function from d_{ntw} to $\widehat{d}_{ntw}$ is

$$\frac{\widehat{d}_{ntw}(s)}{d_{ntw}(s)} = \frac{M_{asp}(s)\,P_{model}(s)\,e^{-sL}}{1 + M_{asp}(s)\,P_{model}(s)\,e^{-sL}}. \quad (6)$$

Then

$$M_{asp}(s) = k_{PMasp} + sk_{DMasp}. \quad (7)$$

Here loop transfer function is

$$G_l(s) = M_{asp}(s)\,P_{model}(s)\,e^{-sL},$$
$$G_l(s) = \left(k_{PMasp} + sk_{DMasp}\right)\left(\frac{K_{tn}}{s\left(J_n s + B_n\right)}\right)e^{-sL} \quad (8)$$

if we rearrange the equations

$$G_l(s) = \left(\frac{k_{PMasp} + sk_{DMasp}}{s}\right)\left(\frac{K_{tn}}{\left(J_n s + B_n\right)}\right)e^{-sL} \quad (9)$$

and define

$$M'_{asp}(s) = \frac{k_{PMasp} + sk_{DMasp}(s)}{s} = k'_{PMasp} + \frac{k'_{IMasp}}{s}, \quad (10)$$
$$P'_{model}(s) = \frac{K_{tn}}{\left(J_n s + B_n\right)}e^{-sL},$$

where $k'_{IMasp} = k_{PMasp}$ and $k'_{PMasp} = k_{DMasp}$.

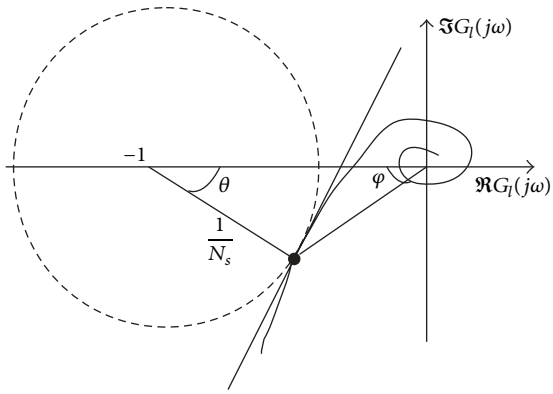

Figure 4: Nyquist diagram of loop function.

Due to the PD-PI relation above, it is possible to design a PD controller for the position control problem under consideration, using the guidelines of the PI design in [29] given based on the system's sensitivity requirements dictated by N_s and derived for a velocity control system, different from our position control system:

$$k_{\mathrm{DMasp}} = \frac{1}{L}\left(1.451 - \frac{1.508}{N_s}\right)\frac{J_n}{K_{tn}},$$
$$k_{\mathrm{PMasp}} = \frac{1}{L}\left(1.451 - \frac{1.508}{N_s}\right)\frac{B_n}{K_{tn}}. \tag{11}$$

Here, N_s is determined by the desired sensitivity specification and is defined as

$$N_s = \max_{0\le\omega<\infty}\frac{1}{L}\left|\frac{1}{1 + P_{\mathrm{model}}(j\omega)\,M(j\omega)}\right|. \tag{12}$$

N_s can also be defined as the inverse of the shortest distance of the open loop transfer function from the Nyquist curve as seen in Figure 4. The major advantages of N_s are that by selecting N_s, performance factors

$$A_m > \frac{N_s}{N_s - 1}$$
$$\varphi_m > 2\arcsin\frac{1}{2N_s} \tag{13}$$

can be constructed. Here, A_m denotes gain margin and φ denotes phase margin.

Reasonable values of the N_s are in the range of 1.3 to 2.

Alternatively, Ziegler-Nichols [30] and Astrom-Hagglund [31] methods can also be used for the design of the $M_{\mathrm{asp}}(s)$ controller.

4.2. Design of Sliding Mode Observer on Master Side. The developed sliding mode observer (SMO) aims to estimate the actual slave position and velocity in the face of the network delay encountered in the feedback loop. This delay is now constant with the use of the delay regulator, which is demonstrated to significantly improve the performance of the SMO compared to past studies of the authors, together with the use of the proposed model following controller. The observer (on the master side) takes into account the following slave model, the outputs of which are fed to the master as slave feedback with the assumption that the actual slave system will track the model closely with the designed MTC.

The model of the slave plant is

$$\dot\theta_{\mathrm{slvmdl}}(t) = \omega_{\mathrm{slvmdl}}(t),$$
$$\dot\omega_{\mathrm{slvmdl}}(t) = \frac{K_{tn}}{J_n}u_{\mathrm{slv}}(t) - \frac{B_n}{J_n}\omega_{\mathrm{slvmdl}}(t). \tag{14}$$

The master side observer designed for the slave has the following form:

$$\dot\theta_e(t) = \omega_e(t)$$
$$\dot\omega_e(t) = \frac{K_{tn}}{J_n}u_{\mathrm{slv}}(t) - \frac{B_n}{J_n}\omega_e(t) + u_o(t). \tag{15}$$

$X = [\theta_e \ \ \omega_e]^T$ are observer states. u_o is control input of the observer (to be determined based on SM theory).

Slave states measured on the master side which is the output of delay regulator are $\theta_{\mathrm{dlyregout}}$, $\omega_{\mathrm{dlyregout}}$:

$$\theta_{\mathrm{dlyregout}}(kT) = \theta_{\mathrm{slvmdl}}(kT - L),$$
$$\omega_{\mathrm{dlyregout}}(kT) = \omega_{\mathrm{slvmdl}}(kT - L), \tag{16}$$

where L is the regulated delay.

The control input applied to the slave also deviates from the actual control input by the same delay as

$$u_{\mathrm{slv}}(kT) = u_{\mathrm{mst}}(kT - L). \tag{17}$$

Next, for the design of the observer, the sliding manifold is selected as

$$\sigma(t) = c_{\mathrm{smo}}e_{\mathrm{smo}}(t) + \dot e_{\mathrm{smo}}(t), \tag{18}$$

where $e_{\mathrm{smo}}(t)$ and $\dot e_{\mathrm{smo}}(t)$ are as follows:

$$e_{\mathrm{smo}}(t) = \theta_{\mathrm{dlyregout}}(t) - \theta_e(t - L),$$
$$\dot e_{\mathrm{smo}}(t) = \omega_{\mathrm{dlyregout}}(t) - \omega_e(t - L). \tag{19}$$

With a properly selected Lyapunov candidate, a control will be designed for the SM based observer that will force the observed states, $\theta_e(kT - L)$ and $\omega_e(kT - L)$, to the measured $\theta_{\mathrm{dlyregout}}$, $\omega_{\mathrm{dlyregout}}$. As given in (16), this actually indicates that the actual slave state values (before the delay) have been reached for use in the master controller.

The Lyapunov candidate and its derivative are selected as follows to satisfy the following conditions:

$$V(t) = \sigma^2(t), \tag{20}$$

$$\dot V(t) = \sigma(t)\,\dot\sigma(t) = -d_{\mathrm{smo}}\sigma^2(t), \tag{21}$$

where

$$\dot\sigma(t) = c_{\mathrm{smo}}\dot e_{\mathrm{smo}}(t) + \dot\omega_{\mathrm{dlyregout}}(t) - \dot\omega_e(t - L). \tag{22}$$

Equations (21) and (22) are used to derive the SM control law as follows [12]:

$$\dot\sigma(t) = -\,d_{\mathrm{smo}}\sigma(t). \tag{23}$$

By substituting (14), (15), and (18) into (22),

$$\dot{\sigma}(t) = c_{\text{smo}}\dot{e}_{\text{smo}}(t) + \dot{\omega}_{\text{dlyregout}}(t) - \frac{K_{tn}}{J_n}u_{\text{mst}}(t-L) + \frac{B_n}{J_n}\omega_e(t-L) - u_o(t). \tag{24}$$

Next, we define

$$\left[u_o(t)\right]_{\text{eq}} = c_{\text{smo}}\dot{e}_{\text{smo}}(t) + \dot{\omega}_{\text{dlyregout}}(t) + \frac{B_n}{J_n}\omega_e(t-L) - \frac{K_{tn}}{J_n}u_{\text{mst}}(t-L) \tag{25}$$

which converts (24) into

$$\dot{\sigma}(t) = \left[u_o(t)\right]_{\text{eq}} - u_o(t). \tag{26}$$

If $u_o(t) = [u_o(t)]_{\text{eq}}$, then $\dot{\sigma} = 0$, and per (23), $\sigma = 0$.

To calculate the observer control, we discretize $\dot{\sigma}$ under the assumption of a very high sampling rate; hence, (26) becomes

$$u_o(kT-T) - \left[u_o(kT-T)\right]_{\text{eq}} = \frac{\sigma(kT) - \sigma(kT-T)}{T} \tag{27}$$

and also

$$u_0(kT) - \left[u_o(kT)\right]_{\text{eq}} = -d_{\text{smo}}\sigma(kT). \tag{28}$$

Assuming that $[u_o(k)]_{\text{eq}}$ does not change between two sampling periods,

$$\left[u_o(kT)\right]_{\text{eq}} = \left[u_o(kT-T)\right]_{\text{eq}}. \tag{29}$$

By rearranging (28) and subtracting from (27) we get

$$u_o(k) = u_o(k-1) + \left[\frac{\left(1 + d_{\text{smo}}T\right)\sigma(k) - \sigma(k-1)}{T}\right]. \tag{30}$$

The control in (30) will enforce the sliding mode to the selected manifold. With the application of this control, and with the consideration of

$$\left[u_o(t)\right]_{\text{eq}} = c_{\text{smo}}\dot{e}_{\text{smo}}(t) + \dot{\omega}_{\text{dlyregout}}(t) + \frac{B_n}{J_n}\omega_e(t-L) - \frac{K_{tn}}{J_n}u_{\text{mst}}(t-L). \tag{31}$$

The observer system in (15) can be rewritten as

$$\begin{aligned}\dot{\theta}_e(t-L) &= \omega_e(t-L),\\ \dot{\omega}_e(t-L) &= -\frac{B_n}{J_n}\omega_e(t-L) + \frac{K_{tn}}{J_n}u_{\text{mst}}(t-L) + c_{\text{smo}}\dot{e}_{\text{smo}}(t) + \dot{\omega}_{\text{dlyregout}}(t) + \frac{B_n}{J_n}\omega_e(t-L) - \frac{K_{tn}}{J_n}u_{\text{mst}}(t-L),\end{aligned} \tag{32}$$

which yields

$$\underbrace{\left[\dot{\omega}_{\text{dlyregout}}(t) - \dot{\omega}_e(t-L)\right]}_{\ddot{e}_{\text{smo}}(t)} + c_{\text{smo}}\dot{e}_{\text{smo}}(t) = 0. \tag{33}$$

Inspecting (23), it can be said that when $\dot{\sigma}(t) \to 0$ $\sigma(t) \to 0$. This indicates that $\dot{e}_{\text{smo}}(t) \to 0$, $c_{\text{smo}}e_{\text{smo}}(t) \to 0$; that is,

$$\begin{aligned}\omega_e(t-L) &= \omega_{\text{dlyregout}}(t) = \omega_{\text{slvmdl}}(t-L),\\ \theta_e(t-L) &= \theta_{\text{dlyregout}}(t) = \theta_{\text{slvmdl}}(t-L).\end{aligned} \tag{34}$$

Block diagram of described Sliding Mode Observer is seen in Figure 5.

5. Design of Model Tracking Control Scheme on Slave Side

In this section, the design of the proposed model tracking control (MTC) is discussed. The MTC based slave control system forces the actual slave system to track a desired slave model, hence achieving disturbance rejection in the face of parameter and load uncertainties. This model tracking scheme is represented in Figure 6 [32, 33]. It should be noted that the slave feedback used on the master side is the output of the slave "model," not the output of the actual slave. Integrated master-slave system is the output of the model system. The use of this model on both master and slave sides is an approach taken in this study that significantly improves master-slave tracking performance. With this approach, the master and slave controllers can also be designed separately.

To derive the model tracking controller, $C_{\text{mtc}}(s)$, the mathematical model of the actual plant, $P_{\text{slv}}(s)$, in (2) is taken into consideration in the following form:

$$\frac{K_t}{J}\left(u_{\text{slv}} + u_{\text{aux}}\right) - \frac{T_L}{J} - \frac{B}{J}\omega_{\text{slvact}} = \dot{\omega}_{\text{slvact}}, \tag{35}$$

where T_L is load torque [Nm], J is total moment of inertia [kg m^2], B is total viscous friction coefficient [Nm s/ rd], ω_{slvact} is angular velocity [rd /s], K_t is torque constant [Nm/A], u_{slv} is control input to track the known part of the slave model, and u_{aux} is control input to compensate for slave model uncertainties.

The model below represents the known portion of the slave model:

$$\frac{K_{tn}}{J_n}u_{\text{slv}} - \frac{B_n}{J_n}\omega_{\text{slvmdl}} = \dot{\omega}_{\text{slvmdl}}, \tag{36}$$

where all values reflect the known slave model parameters and variables, as below:

J_n is moment of inertia of slave model [kg m^2];

B_n is viscous friction coefficient of slave model [Nm s/ rd];

ω_{slvmdl} is angular velocity [rd /s];

K_{tn} is torque constant [Nm/A].

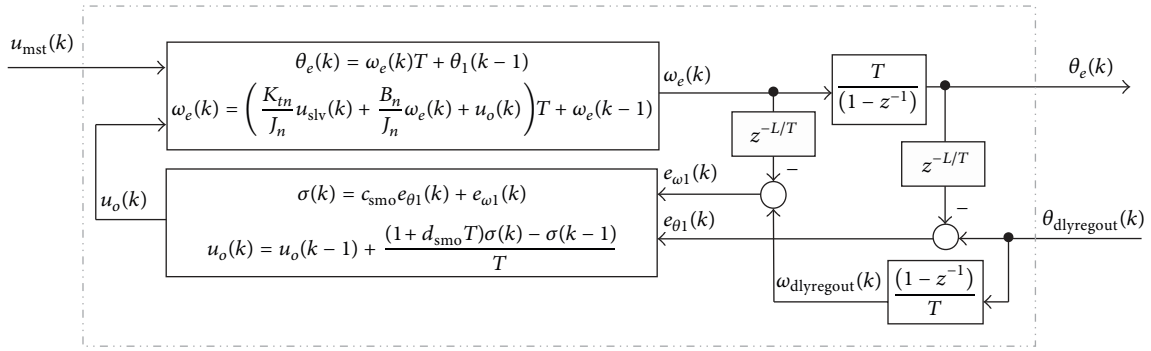

Figure 5: Diagram of sliding mode observer.

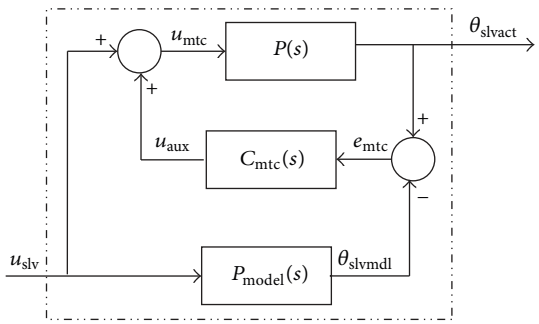

Figure 6: Architecture of model tracking control at slave side.

With the aim of deriving the appropriate tracking controller, C_{mtc}, first the error between the actual plant and model plant outputs should be defined as

$$\begin{aligned} e_{\text{mtc}} &= \theta_{\text{slvact}} - \theta_{\text{slvmdl}}, \\ \dot{e}_{\text{mtc}} &= \omega_{\text{slvact}} - \omega_{\text{slvmdl}}, \\ \ddot{e}_{\text{mtc}} &= \dot{\omega}_{\text{slvact}} - \dot{\omega}_{\text{slvmdl}}. \end{aligned} \tag{37}$$

Using (35) and (36), the second derivative of the error is defined as

$$\begin{aligned} \ddot{e}_{\text{mtc}} = {} & \frac{-K_{tn}}{J_n}u_{\text{slv}} + \frac{B_n}{J_n}\omega_{\text{slvmdl}} + \frac{K_t}{J}\left(u_{\text{slv}} + u_{\text{aux}}\right) \\ & - \frac{T_L}{J} - \frac{B}{J}\omega_{\text{slvact}}. \end{aligned} \tag{38}$$

Defining the error between actual and model parameter values with the symbol Δ as

$$\frac{k_t}{J} = \frac{k_{tn}}{J_n} + \Delta\left(\frac{k_t}{J}\right) \qquad \frac{B}{J} = \frac{B_n}{J_n} + \Delta\left(\frac{B}{J}\right) \tag{39}$$

can be reorganized as below:

$$\begin{aligned} & \ddot{e}_{\text{mtc}} \\ & = \frac{K_{tn}}{J_n}\left(-u_{\text{slv}} + u_{\text{slv}} + u_{\text{aux}}\right) + \Delta\left(\frac{K_t}{J}\right)\left(u_{\text{slv}} + u_{\text{aux}}\right) \\ & \quad - \frac{B_n}{J_n}\dot{e}_{\text{mtc}} - \Delta\left(\frac{B}{J}\right)\omega_{\text{slvact}} - \frac{T_L}{J}, \end{aligned} \tag{40}$$

$$\begin{aligned} & \ddot{e}_{\text{mtc}} + \frac{B_n}{J_n}\dot{e}_{\text{mtc}} \\ & = \frac{K_{tn}}{J_n}u_{\text{aux}} - \frac{T_L}{J} \\ & \quad + \Delta\left(\frac{K_t}{J}\right)\left(u_{\text{slv}} + u_{\text{aux}}\right) - \Delta\left(\frac{B}{J}\right)\omega_{\text{slvact}}. \end{aligned} \tag{41}$$

Next, the load and parameter uncertainties are defined as d_{mtc}

$$\frac{1}{J_n}d_{\text{mtc}} \triangleq \frac{T_L}{J} - \Delta\left(\frac{K_t}{J}\right)\left(u_{\text{slv}} + u_{\text{aux}}\right) + \Delta\left(\frac{B}{J}\right)\omega_{\text{slvact}}. \tag{42}$$

Here disturbance upper bound can also be defined as

$$\begin{aligned} \left[d_{\text{mtc}}\right]_{\max} = {} & \frac{J_n\left[T_L\right]_{\max}}{[J]_{\min}} - J_n\left[\Delta\left(\frac{K_t}{J}\right)\right]_{\max}\left[u_{\text{mtc}}\right]_{\max} \\ & + J_n\left[\Delta\left(\frac{B}{J}\right)\right]_{\max}\left[\omega_{\text{slvact}}\right]_{\max}. \end{aligned} \tag{43}$$

Equation (42) when substituted in (41) will yield the following error dynamics:

$$\ddot{e}_{\text{mtc}} + \frac{B_n}{J_n}\dot{e} = \frac{1}{J_n}\left(K_{tn}u_{\text{aux}} - d_{\text{mtc}}\right). \tag{44}$$

Inspecting (44), it could be observed that when

$$u_{\text{aux}} \longrightarrow \frac{d_{\text{mtc}}}{K_{tn}}, \qquad \dot{e}_{\text{mtc}} \longrightarrow 0 \quad \text{while } e_{\text{mtc}} \longrightarrow \text{constant}. \tag{45}$$

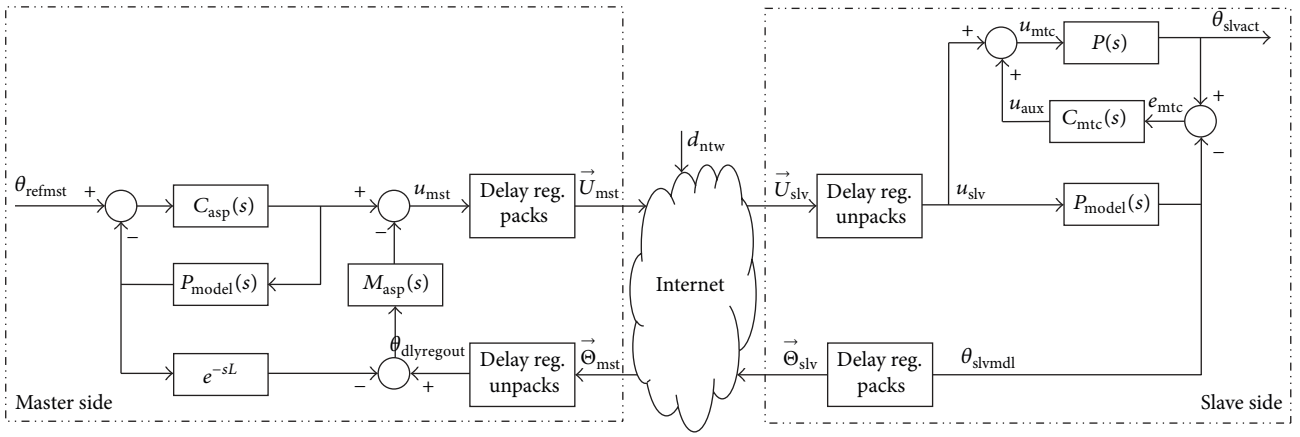

Figure 7: Modified SP and MTC based master-slave configuration.

For $e_{\text{mtc}} \rightarrow 0$, the following error dynamics should be derived:

$$\ddot{e}_{\text{mtc}} + \frac{B_n}{J_n}\dot{e}_{\text{mtc}} + k_{\text{mtc}}e_{\text{mtc}} = 0. \tag{46}$$

This condition requires the following term:

$$\frac{1}{J_n}\left(K_{tn}u_{\text{aux}} - d_{\text{mtc}}\right) = -k_{\text{mtc}}e_{\text{mtc}} \tag{47}$$

which results in the following relationships:

$$d_{\text{mtc}} = k_{tn}u_{\text{aux}} + k_{\text{mtc}}J_n e_{\text{mtc}}, \tag{48}$$

$$u_{\text{aux}} = \frac{d_{\text{mtc}} - k_{\text{mtc}}J_n e_{\text{mtc}}}{K_{tn}}. \tag{49}$$

Define a new variable z as

$$z \triangleq d_{\text{mtc}} - k_{\text{mtc}}J_n e \longrightarrow d = z + k_{\text{mtc}}J_n e_{\text{mtc}}. \tag{50}$$

Assume that d_{mtc} has a very slow variation:

$$\dot{z} = -k_{\text{mtc}}J_n\dot{e}_{\text{mtc}} \qquad \ddot{z} = -k_{\text{mtc}}J_n\ddot{e}_{\text{mtc}}. \tag{51}$$

Rewrite (44) in terms of z:

$$\ddot{z} + \frac{B_n}{J_n}\dot{z} + k_{\text{mtc}}z = k_{\text{mtc}}d_{\text{mtc}}. \tag{52}$$

Hence

$$\ddot{z} + \frac{B_n}{J_n}\dot{z} + k_{\text{mtc}}z = k_{\text{mtc}}\left(k_{\text{mtc}}J_n e_{\text{mtc}} + K_{tn}u_{\text{aux}}\right). \tag{53}$$

To derive $C_{\text{mtc}}(s)$, z in (53) is expressed in s-domain:

$$z(s) = \frac{k_{\text{mtc}}}{s^2 + \left(B_n/J_n\right)s + k_{\text{mtc}}}\left(k_{\text{mtc}}J_n e_{\text{mtc}} + K_{tn}u_{\text{aux}}\right) \tag{54}$$

which is substituted in d_{mtc} expression, yielding

$$d_{\text{mtc}} = \frac{k_{\text{mtc}}}{s^2 + \left(B_n/J_n\right)s + k_{\text{mtc}}}\left(k_{\text{mtc}}J_n e_{\text{mtc}} + K_{tn}u_{\text{aux}}\right) + k_{\text{mtc}}J_n e_{\text{mtc}}. \tag{55}$$

Replacing d_{mtc} with its definition in (48),

$$K_{tn}u_{\text{aux}} = \frac{k_{\text{mtc}}}{s^2 + \left(B_n/J_n\right)s + k_{\text{mtc}}}\left(k_{\text{mtc}}J_n e_{\text{mtc}} + K_{tn}u_{\text{aux}}\right) + k_{\text{mtc}}J_n e_{\text{mtc}} - k_{\text{mtc}}J_n e_{\text{mtc}}. \tag{56}$$

Expressing (56) in terms of aux, the expression for the tracking control, $C_{\text{mtc}}(s)$, can be derived as follows:

$$\left(s^2 + \frac{B_n}{J_n}s + k_{\text{mtc}}\right)K_{tn}u_{\text{aux}} = k_{\text{mtc}}K_{tn}u_{\text{aux}} + k_{\text{mtc}}J_n\left(k_{\text{mtc}}e_{\text{mtc}}\right),$$
$$u_{\text{aux}} = \underbrace{\frac{J_n k_{\text{mtc}}^2}{s^2 + \left(B_n/J_n\right)s}}_{C_{\text{mtc}}(s)}e_{\text{mtc}}(s). \tag{57}$$

Here, the controller, $C_{\text{mtc}}(s)$, is configured as a compensator and its output is added onto the PD control generated, which is the constant time delayed version of the control signal generated on the master side.

6. Experimental Results with Proposed Methods for the Two Master-Slave Configurations

In this section, experimental results will be provided with the proposed schemes, which are presented as two configurations. The controller parameters are $c_{\text{smo}} = 0.0001$, $d_{\text{smo}} = 0.001$, $k_{\text{PCasp}} = k_{\text{PCsmo}} = 0.92$, $k_{\text{ICasp}} = K_{\text{ICsmo}} = 0.1$, $k_{\text{DCasp}} = k_{\text{DCsmo}} = 2$, $k_{\text{PMasp}} = .03$, $k_{\text{DMasp}} = .12$, and $k_{\text{mtc}} = 200$. Also Figure 7 presents the master-slave configuration based on the modified SP and MTC, abbreviated as SP-MTC for brevity, and Figure 8 presents the master-slave configuration based on the modified SMO and MTC. In both configurations, the developed model tracking controller (MTC) forces the slave to track the desired model, hence avoiding instability issues and increasing tracking accuracy despite parameter uncertainties and disturbances on the slave side. As demonstrated in Figure 2, the control input (a current signal) for

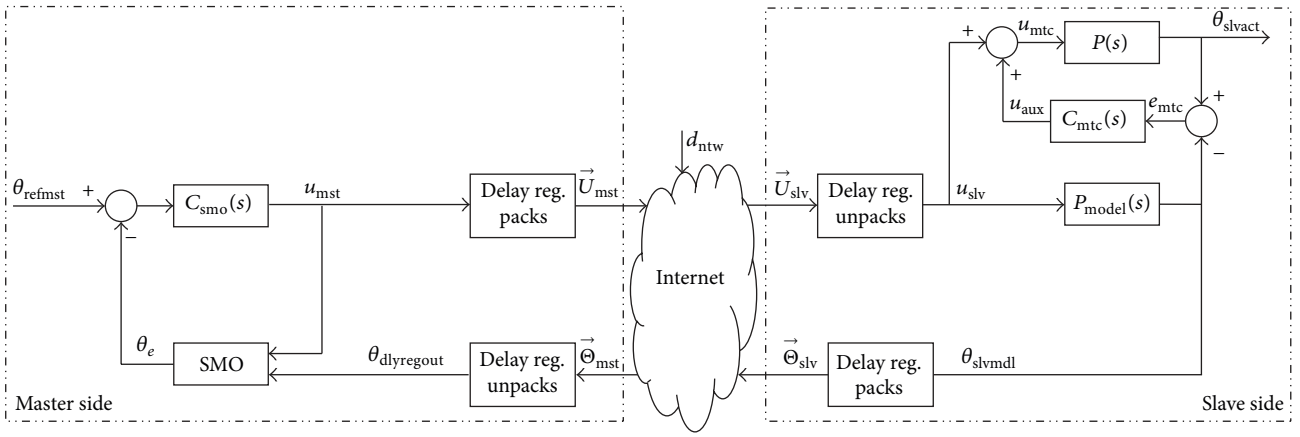

Figure 8: SMO and MTC based master-slave configuration.

the slave side is generated by the master side controller, which takes into consideration the reference trajectory and the slave feedback received from the model. This is an important contribution of this study, as in the previous studies of the authors [13]; it was demonstrated that the use of the actual slave plant feedback causes steady state error and drift in the slave performance.

The experimental results are obtained under random network delays both in the feedback and control loops. For the proper operation of the SMO and ASP schemes, a delay regulator is designed on both master and the slave sides to regulate these random delays to a constant delay value of 400 ms. This value was obtained from the intercontinental network experiments presented in [23]. To further challenge the slave plant, the load disturbance on the slave and the reference trajectories are applied as sinusoidal functions and bidirectional trajectories, respectively, which sometimes gives rise to short spikes.

A direct-drive motor driven single-link arm is used in the experiments, the parameters of which are listed in Table 1. The delay is generated as a random signal varying between 100 and 400 milliseconds.

Figures 9 and 10 represent the performance of the ASP and SMO based configurations, respectively, under no load on the slave. The figures demonstrate the delay effect in all cases. Inspecting the zoomed versions of the diagrams, one may note a slightly smoother performance of ASP based configuration.

Figures 11 and 12 represent the performance of the ASP and SMO based configurations, respectively, under a sinusoidal load variation on the slave side. The figures demonstrate the delay effect in all cases. While a slightly smoother performance is noted with ASP again, both configurations display similar performances in terms of tracking error.

Table 1: Experiment parameters.

Parameter name	Parameter value	Description
V_{qn}	60 V	Motor nominal voltage
i_{qn}	5 A	Motor nominal current
R_q	0.6 Ω	Motor phase windings resistance
L_q	0.005 H	Motor phase windings inductance
K_b	2.3 Vsec/rad	Back e.m.f. constant
T_{en}	10 Nm	Motor nominal torque
K_{vi}	1 A/V	Motor driver gain
ω_n	4 πrad/sec	Motor nominal speed
T_{em}	15 Nm	Motor maximum torque
K_t	2 Nm/A	Torque constant
J	0.012 kg-m^2	Effective inertia
B	0.207 Nms/rad	Effective viscous friction
T_L	10 sin ΘNm	Load torque

7. Conclusions and Future Directions

This study builds on the disturbance observer based approach in bilateral control and contributes to significant improvements in both control and communication issues faced with position control aspects of bilateral control systems. To this aim, two novel master-slave configurations are proposed: one based on a sliding-mode observer and model-tracking controller and the other based on Astrom's Smith predictor on the master side. Both configurations benefit from a delay regulator, which regulates the random network delay into a constant delay. Both configurations also use a MTC designed for the slave side disturbance rejection and trajectory tracking.

Experiments are conducted on a single-link arm system under variable gravitational effects and a randomly varied network delay of 100–400 ms that impacts both the feedback and control loop. While the ASP is a more capable version of the standard SP against disturbances stemming from network and slave uncertainties, the much reduced system uncertainties via the proposed combination of the delay regulator and MTC contribute significantly to the overall performance.

The delay regulator and MTC have also benefited the SMO based configuration significantly, which has been

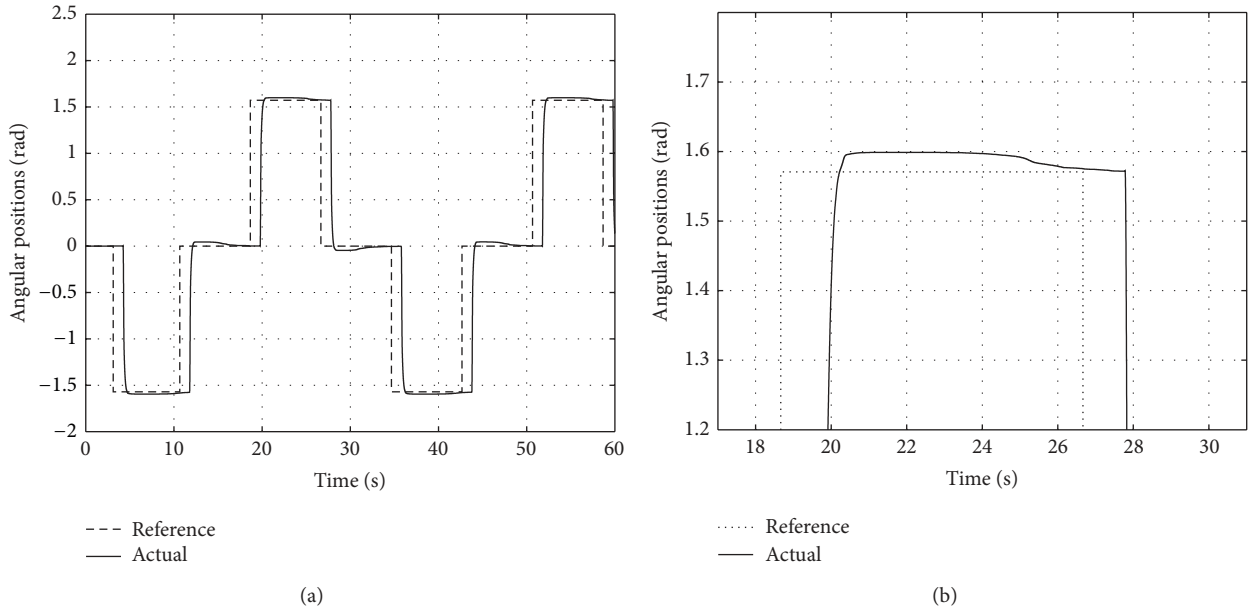

Figure 9: (a) Reference tracking performance of slave with the ASP based configuration under no load (delay effect displayed); (b) zoomed version of performance.

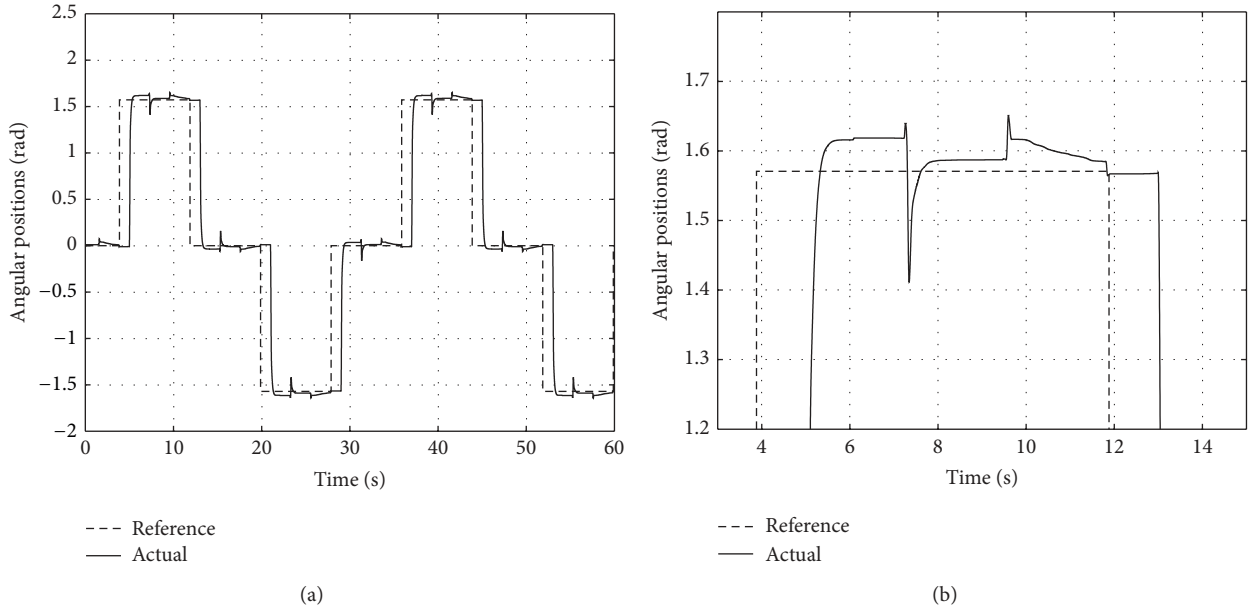

Figure 10: (a) Reference tracking performance of slave with the SMO based configuration under no load (delay effect displayed); (b) zoomed version of performance.

shown to demonstrate a poor tracking performance under variable network and slave disturbances in the authors' previous studies, while achieving perfect tracking under no load and constant network delay. Hence, both configurations demonstrate a significantly improved tracking performance against model-mismatch and randomly varying network delay (within 100–400 ms) and can handle feedback loop deteriorations arising from the limited buffer size of the delay regulator. However, currently neither of the configurations can handle network delays exceeding 400 ms in the control loop. This issue requires further attention and will be addressed in the authors' future papers.

Conflict of Interests

The authors declare that there is no conflict of interests regarding the publication of this paper.

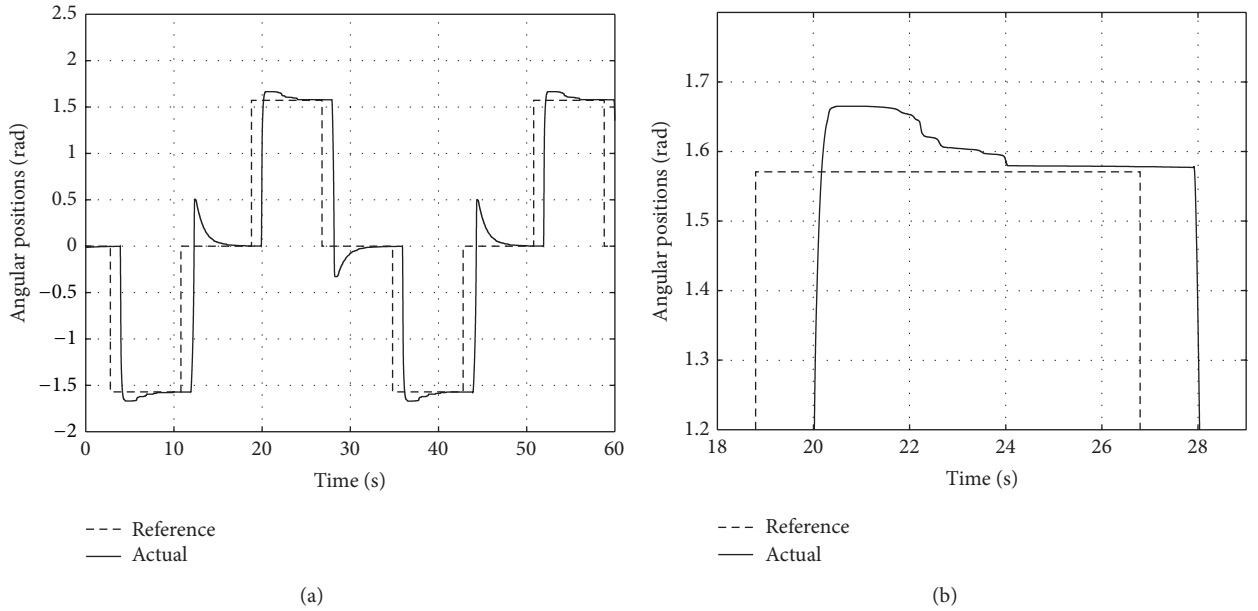

Figure 11: (a) Reference tracking performance of slave with the ASP based configuration under sinusoidal disturbance (delay effect displayed); (b) zoomed version of performance.

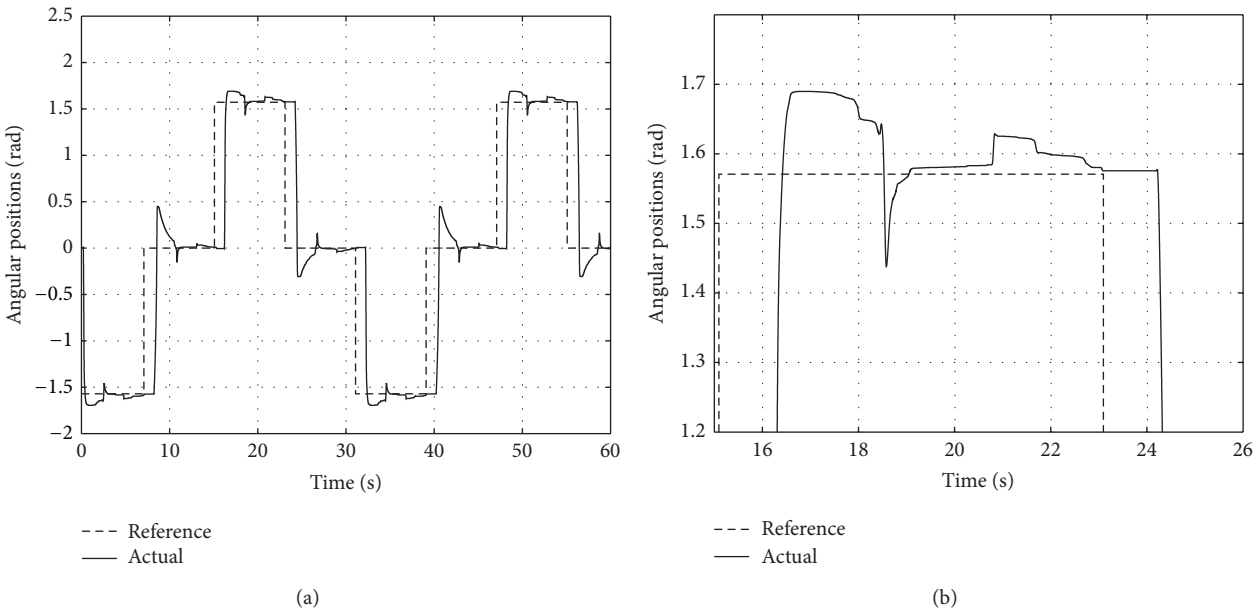

Figure 12: (a) Reference tracking performance of slave with the SMO based configuration under sinusoidal load (delay effect displayed); (b) zoomed version of performance.

Acknowledgments

This study has been supported by the National Science Foundation-Computer & Information Sciences and Engineering (NSF-CISE) and NSF Office of International Science & Engineering (NSF-OISE).

References

[1] M. Li, H. Liu, A. Jiang et al., "Intra-operative tumour localisation in robot-assisted minimally invasive surgery: a review," *Proceedings of the Institution of Mechanical Engineers, Part H: Journal of Engineering in Medicine*, vol. 228, no. 5, pp. 509–522, 2014.

[2] T. Mori, "Modified bilateral control by using intervention impedance based on passivity of flexible master-slave manipulators and its design methods," in *Proceedings of the 12th International Conference on Control, Automation and Systems (ICCAS '12)*, pp. 748–753, October 2012.

[3] S. Munir and W. Book, "Wave-based teleoperation with prediction," in *Proceedings of the American Control Conference*, vol. 6, pp. 4605–4611, 2001.

[4] G. M. H. Leung, B. A. Francis, and J. Apkarian, "Bilateral controller for teleoperators with time delay via μ-synthesis," *IEEE Transactions on Robotics and Automation*, vol. 11, no. 1, pp. 105–116, 1995.

[5] D. Yashiro and K. Ohnishi, "L^2 stable four-channel control architecture for bilateral teleoperation with time delay," in *Proceedings of the 10th IEEE International Workshop on Advanced Motion Control (AMC '08)*, pp. 324–329, Trento, Italy, March 2008.

[6] L.-G. García-Valdovinos, V. Parra-Vega, and M. A. Arteaga, "Observer-based sliding mode impedance control of bilateral teleoperation under constant unknown time delay," *Robotics and Autonomous Systems*, vol. 55, no. 8, pp. 609–617, 2007.

[7] D. Yashiro and K. Ohnishi, "Multirate sampling method for bilateral control with communication bandwidth constraint," in *Proceedings of the IEEE International Conference on Industrial Technology (ICIT '09)*, February 2009.

[8] Y. Cheung and J. Chung, "Cooperative control of a multi-arm system using semi-autonomous telemanipulation and adaptive impedance," in *Proceedings of the International Conference on Advanced Robotics (ICAR '09)*, pp. 1–7, June 2009.

[9] S. Arai, K. Miyake, T. Miyoshi, and K. Terashima, "Bilateral telecontrol using mullti-fingered humanoid root an with communication delay," in *Proceedings of the SICE Annual Conference*, pp. 711–715, 2008.

[10] V. T. Minh and F. M. Hashim, "Adaptive teleoperation system with neural network-based multiple model control," *Mathematical Problems in Engineering*, vol. 2010, Article ID 592054, 15 pages, 2010.

[11] C.-C. Hua, Y. Yang, and X. Guan, "Neural network-based adaptive position tracking control for bilateral teleoperation under constant time delay," *Neurocomputing*, vol. 113, pp. 204–212, 2013.

[12] B. Gadamsetty, S. Bogosyan, M. Gokasan, and A. Sabanovic, "Novel observers for compensation of communication delay in bilateral control systems," in *Proceedings of the 35th Annual Conference of the IEEE Industrial Electronics Society (IECON '09)*, pp. 3019–3026, November 2009.

[13] B. Gadamsetty, S. Bogosyan, M. Gokasan, and A. Sabanovic, "Sliding mode and EKF observers for communication delay compensation in bilateral control systems," in *Proceedings of the IEEE International Symposium on Industrial Electronics (ISIE '10)*, pp. 328–333, July 2010.

[14] W. Shen, J. Gu, and Z. Feng, "A stable tele-robotic neurosurgical system based on SMC," in *Proceedings of the IEEE International Conference on Robotics and Biomimetics (ROBIO '07)*, pp. 150–155, Sanya, China, December 2007.

[15] L.-C. Hung, C.-Y. Wang, and H.-Y. Chung, "Sliding mode control for uncertain time-delay systems with sector nonlinearities via fuzzy rule," in *Proceedings of the IEEE International Conference on Systems, Man and Cybernetics*, vol. 1, pp. 251–256, 2005.

[16] X. Yu, Q. Han, X. Li, and C. Wang, "Time-delay effect on equivalent control based single-input sliding mode control systems," in *Proceedings of the IEEE 10th International Workshop on Variable Structure Systems (VSS '08)*, pp. 13–17, June 2008.

[17] L. G. Garcia-Valdovinos, V. Parra-Vega, and M. A. Arteaga, "Observer-based higher-order sliding mode impedance control of bilateral teleoperation under constant unknown time delay," in *Proceedings of the IEEE/RSJ International Conference on Intelligent Robots and Systems (IROS '06)*, pp. 1692–1699, October 2006.

[18] A. Šabanović, M. Elitas, and K. Ohnishi, "Sliding modes in constrained systems control," *IEEE Transactions on Industrial Electronics*, vol. 55, no. 9, pp. 3332–3339, 2008.

[19] O. J. Smith, "A controller to overcome dead time," *ISA Journal*, vol. 6, no. 2, pp. 28–33, 1959.

[20] K. Astrom, C. C. Hang, and B. C. Lim, "A new Smith predictor for controlling a process with an integrator and long dead-time," *IEEE Transactions on Automatic Control*, vol. 39, no. 2, pp. 343–345, 1994.

[21] K. Natori, R. Oboe, and K. Ohnishi, "Stability analysis and practical design procedure of time delayed control systems with communication disturbance observer," *IEEE Transactions on Industrial Informatics*, vol. 4, no. 3, pp. 185–197, 2008.

[22] K. Natori and K. Ohnishi, "A design method of communication disturbance observer for time-delay compensation, taking the dynamic property of network disturbance into account," *IEEE Transactions on Industrial Electronics*, vol. 55, no. 5, pp. 2152–2168, 2008.

[23] K. Matsuo, T. Miura, and T. Taniguchi, "A speed control method of small DC motor through IP network considering packet loss," *IEEJ Transactions on Electrical and Electronic Engineering*, vol. 2, no. 6, pp. 657–659, 2007.

[24] S. Munir and W. J. Book, "Internet-based teleoperation using wave variables with prediction," *IEEE/ASME Transactions on Mechatronics*, vol. 7, no. 2, pp. 124–133, 2002.

[25] A. Kuzu, S. Bogosyan, and M. Gokasan, "Network in the loop platform for research and training in bilateral control," in *Proceedings of the 12th IEEE International Workshop on Advanced Motion Control (AMC '12)*, pp. 1–6, Sarajevo, Bosnia and Herzegovina, March 2012.

[26] K. Watanabe and M. Ito, "A process-model control for linear systems with delay," *IEEE Transactions on Automatic Control*, vol. 26, no. 6, pp. 1261–1269, 1981.

[27] Y. D. Chen, P. C. Tung, and C. C. Fuh, "Modified Smith predictor scheme for periodic disturbance reduction in linear delay systems," *Journal of Process Control*, vol. 17, no. 10, pp. 799–804, 2007.

[28] W. D. Zhang and Y. X. Sun, "Modified smith predictor for controlling integrator/time delay processes," *Industrial and Engineering Chemistry Research*, vol. 35, no. 8, pp. 2769–2772, 1996.

[29] Y.-G. Wang, H.-H. Shao, and J. Wang, "PI tuning for processes with large dead time," in *Proceedings of the American Control Conference*, vol. 6, pp. 4274–4278, June 2000.

[30] J. G. Ziegler and N. B. Nichols, "Optimum settings for automatic controllers," *Journal of Dynamic Systems, Measurement, and Control*, vol. 115, no. 2B, pp. 220–222, 1993.

[31] K. J. Åström, T. Hägglund, C. C. Hang, and W. K. Ho, "Automatic tuning and adaptation for PID controllers—a survey," *Control Engineering Practice*, vol. 1, no. 4, pp. 699–714, 1993.

[32] F. Leonardi and J. Da Cruz, "Robust model tracking and 2-d control design," in *Proceedings of the 10th Mediterranean Conference on Control and Automation*, 2002.

[33] A. Kuzu, S. Bogosyan, M. Gokasan, and A. Sabonovic, "Control and measurement delay compensation in bilateral position control," in *Proceedings of the IEEE International Conference on Mechatronics (ICM '11)*, pp. 1003–1010, April 2011.